6B.6 NEXRAD DIFFERENTIAL REFLECTIVITY CALIBRATION

J.C. Hubbert,* F. Pratte, M. Dixon and R. Rilling
National Center for Atmospheric Research, Boulder CO

1. INTRODUCTION

NCAR (National Center for Atmospheric Research) has been tasked by the Office and Science and Technology (OS&T) of NWS (National Weather Service) to determine the uncertainty of various methods for the calibration of Z_{dr} using S-Pol, NCAR's S-band polarimetric radar. Three techniques are investigated 1) the vertical pointing (VP) technique, 2) the engineering calibration (EC) technique and 3) the crosspolar power (CP) technique (Hubbert et al. 2003). Uncertainty of measurements is a way to quantify the probability that a measurement (in the present case a calculated calibration factor) lies within some error bounds. Thus, the goal of this this project is to quantify the uncertainty of the estimated Z_{dr} calibration factors determined by each method.

Dual polarized radars promise to increase the accuracy of radar rainfall measurements. The copolar differential power measurement, Z_{dr}, as well as the specific differential phase, ϕ_{dp}, contain additional information about the scattering medium that can be used to increase the accuracy of precipitation measurements that are based solely on radar reflectivity. However, to realize this benefit, Z_{dr} should be calibrated to about one tenth of a dB.

One widely accepted way to calibrate Z_{dr} is to point the radar dish vertically in light rain and measure Z_{dr} while turning the dish 360 degrees. Since raindrops have no preferred orientation (i.e., distributed uniform randomly in the plane of polarization) 360-degree-integrated, intrinsic Z_{dr} is zero dB. Thus, any measured non-zero dB Z_{dr} yields the radar system Z_{dr} offset.

A second way to calibrate Z_{dr} is with an EC approach based on engineering measurements (Zrnić et al. 2006). The radar transmit and receive paths are divided into "active" and "passive" parts. The gains and losses of the "passive" or "static" parts, i.e. the waveguides and antenna, are measured by using test signals and radiation from the sun. The gain of the active signal path (i.e., receiver chain) is monitored via test signal injection on a continuous basis. Transmit powers are also monitored. By combining the passive and active calibration measurements, the Z_{dr} bias can be estimated.

In this paper estimated uncertainty of the three Z_{dr} calibration techniques are given. Issues affecting the uncertainty budgets are discussed. Experimental data from NCAR's S-Pol (S-band Polarimetric Radar) are given that indicate the uncertainty of each method.

*NCAR/EOL, Boulder, Colorado 80307, email: hubbert@ucar.edu

2. UNCERTAINTY MEASUREMENT CONCEPTS

Calibration is a measurement process that assigns values to the property of an artifact or to the response of an instrument relative to reference standards or to a designated measurement process. Its purpose is to reduce the bias of the measurement process. There are measurement errors associated with this measurement process. Uncertainty can be defined as an estimate of the expected limits of experimental error. Uncertainty, in general, of measurement arises from incomplete knowledge, control, understanding, and definition of the processes influencing the measurement. Influence effects, such as temperature, humidity, frequency, mechanical stresses, path variations, and mismatches affect the result of measurements. (See http://www.itl.nist.gov/div898/handbook/index.htm for more detailed treatment of calibration and uncertainty).

Uncertainty can be categorized as either Type A or Type B. Type A uncertainty is represented by the standard deviation of a set of measurements and is primarily quantified by repetition under controlled test conditions (sometimes referred to as under statistical control). Type B uncertainty is any other non-measured uncertainty (e.g., manufacturer specifications). Type B uncertainty can also be represented by the standard deviation of an assumed Normal Distribution but is not quantified through measurement.

Errors can also be categorized (modeled) as systematic or random. Systematic measurement errors bias the mean of a measurement data set, i.e., increasing the number of measurements and averaging will not reduce systematic errors as it will random errors. One way to detect and correct for systematic errors is to use a calibration standard, if one exists. Typically, subtle systematic errors are the most difficult to detect, model, quantify and correct. If all systematic errors are eliminated, the remaining fluctuations in a measurement data set are considered random measurement errors and can be quantified by calculation of the standard deviation of the measured data set. The random errors are usually considered Gaussian distributed but this assumption should be examined for each data set. The systematic errors, however, can also be modeled as random Gaussian distributed and included in an uncertainty budget.

An uncertainty specification is incomplete without a confidence interval (Taylor and Kuyatt 1994). The confidence interval used in this paper is 2σ or two standard deviations. This is sometimes referred to as 2σ coverage. The 2σ coverage standard is used in this paper since this is the coverage value typically used by manufactures of RF devices. It also seems reasonable that meteorologist/hydrologists would like to use Z_{dr} measurements that are calibrated to within 0.1 dB with 95% confidence (i.e., 2σ coverage). In fact, the NEXRAD Technical Advisory Committee recently recommended (in March 2007) that Z_{dr} be calibrated to within 0.1 dB with 95% confidence (i.e., 2σ coverage).

The measurements presented in this paper are typically expressed as

$$E = M \pm \delta \tag{1}$$

where E is the quantity estimated, M is the measurement (or mean of measurements) and δ represents the uncertainty of the measurement with 2σ coverage. The desired Z_{dr} calibration goal can be expressed as

$$Z_{dr}^{cal} = Z_{dr}^{m} + Z_{dr}^{bias} \pm \delta \tag{2}$$

where Z_{dr}^{cal} is the corrected or calibrated Z_{dr}, Z_{dr}^{m} is the measured Z_{dr} estimated from radar data, Z_{dr}^{bias} is the Z_{dr} bias calculated via one of the calibration techniques and δ is the 2σ uncertainty of the bias estimate. Note that other possible biases to the Z_{dr}^{cal} estimate that are external to the radar, such as differential propagation attenuation, are not considered here.

Use of automated test equipment, described next, for calibration measurements permits more complete decomposition of Z_{dr} uncertainty and will reduce human error and variance in measurement due to repeated connects and disconnects of RF measurement equipment.

3. AUTOMATED TEST EQUIPMENT (ATE)

Mechanical processes and procedures such as attaching and re-attaching cables, couplers and meters introduce variability to the EC approach. To reduce these effects, Automatic Test Equipment (ATE) has now been built into S-Pol to measure test point signals, inject test signals and monitor environmental variables such as temperature along the signal path using fixed cable attachments and electronic switches. Figure 1 shows a block diagram of S-Pol. The green box shows the ATE with its multiple input and output lines marked in yellow. The shown yellow connectors (small circles) are connected to the other Test Points also marked in yellow. The S-Pol system has two parallel processors: 1) the VIRAQ (developed by NCAR) and 2) the SIGMET RVP8.

The transmit RF signal (red box) goes through a power distribution network which provides for 1) fast alternating H and V polarization transmission (pulse to pulse) via a fast mechanical switch 2) simultaneous H and V transmission via a power divider 3) H only transmission and 4) V only transmission. The transmit signal(s) pass through the circulators, Test Point 3, rotary joints, Test Point 2 and then to the antenna/dish. The received signal passes back through to the circulators and then the LNAs. Physically, the transmitter, the circulators, the LNAs and the remaining receiver and processor circuits are all located in the S-Pol “transmitter trailer”. After demodulation to IF (intermediate frequency), the signals pass through a switch shown in blue. The switch can direct the IF signals to either IF amplifier #1 (called copolar amp.) or IF amplifier #2 (called crosspolar amp.). When operating in fast alternating H and V transmission mode, the switch is typically used to direct the copolar signals to the same IF amplifier so that any temporal variation in the IF amplifier and remaining sections of the receiver/processor will affect both copolar signals equally. This is done to reduce the variance of Z_{dr} measurements. Thus, S-Pol has four separate receiver paths to calibrate: 1) H signal to IF amp #1, 2) H signal to IF amp #2, 3) V signal to IF amp #1, and 4) V signal to IF amp #2. Test Point 4 yields the digitized in phase and quadrature (I and Q) samples (see http://www.eol.ucar.edu/rsf/spol/spol.html for a description of S-Pol).

The ATE consists of a control computer, wideband power meter, signal generator, noise sources, attenuators and an RF switching matrix all of quality necessary to achieve overall 0.1 dB measurement uncertainty. Appropriate control connections are established between the ATE and the digital receiver, transmitter, and antenna pedestal. Shown in Figs. 2 and 3 are photos of some of the ATE components. Fig. 2 shows the HP Multi-Function Switch and Measurement unit, Power Meter, Signal Generator and the rack mount PC which runs LabVIEW. Also seen is the RCP8/RVP8 IO Panel. Fig. 3 shows a large, approximately five feet high, steel circuit plate with switches, power supplies, an attenuator, a power sensor and control circuitry for the ATE. Distributed along the electrical paths are temperature sensors which are also connected to the PC. Via the PC, test signal are injected and powers are monitored and temperatures are recorded.

a. *ATE measurements*

In the following plots a constant signal is injected at measurement plane 3 (see Fig. 7) and the signal is monitored at test plane four (the I&Q values). Sown in Fig. 4 is the H channel copolar power versus time in fractional days (about 4 hours total). The maximum power excursion is about 0.65 dBm. The oscillating behavior is a result of temperature fluctuations in the S-Pol transmitter trailer cause by air-conditioner cycling. Fig. 5 shows the H-copolar power minus V-crosspolar power versus time. The effect of cycling of the air-conditioner is clearly visible. The maximum power excursion is about 0.018 dBm. There is trend seen in the data in the second half of the plot that indicates a possible small change in Z_{dr} bias. The question naturally arises as to what is the cause of this Z_{dr} drift. To investigate this question, plots such as shown in Fig. 6 can be constructed. Shown in Fig. 6 the the H-copolar power minus the H-crosspolar power as a function of IFD temperature. The data correlation seen indicates that the temperature drift of the IFD is at least part of cause of the data trend seen in Fig. 6 . Such analysis provides the capability to identify components and factors that cause Z_{dr} bias drifts.

The temperature versus power transfer functions have been experimentally determined for the major components of the receiver chain, e.g., the IFDs, the LNAs, etc. We have found that if such corrections are applied to Z_{dr} calibration measurements, the uncertainty of the measurements can be reduced by about a factor of 2.

4. ENGINEERING CALIBRATION APPROACH

The essence of the EC method can be understood via Fig. 7. The blue lines represent measurements planes where signal can be either injected or measured by the ATE. The principle behind all of the calibration techniques is to measure the differential path losses 1) from the transmitter out through the antenna and 2) from outside the antenna back through to the received I and Q samples. Note that the path from the circulators through the antenna is common to both transmit and receive paths. It can be shown that the following calibration equation accounts for the entire electrical transmit and receive paths. The EC Z_{dr} calibration equation is,

$$Z_{dr}^{bias} = \Delta(1,2)_{pulse} + 2\Delta(S,4)_{noise} - \Delta(2,4)_{noise}. \quad (3)$$

where the terms are in dB and the number pairs (and the letter S) correspond to the measurement planes shown in Fig. 7. The $\Delta(1,2)_{pulse}$ term is a measurement of the differential path loss from the transmitter to measurement plane 2. Physically, the radar transmit pulses are monitored at measurement plane 1 and RF power measurements are made at plane 2 via a waveguide coupler. The term $\Delta(S,4)_{noise}$ determines the differential gain from outside the antenna to the I and Q samples using the sun as an unpolarized RF source (i.e., the H and V power from the sun are equal, a very good assumption (Tapping 2001)). The $\Delta(2,4)_{noise}$ term is measured by injecting noise at measurement plane 2 and measuring the resulting differential power at measurement plane 4 via the I and Q samples. In this way, the system Z_{dr}^{bias} is measured. Thus, to determine the uncertainty of this Z_{dr} bias estimate is tantamount to determining the Z_{dr} uncertainty of each term on the right hand side of Eq. (3) in conjunction with each other.

The Type A uncertainty of a particular repeated RF power measurement (i.e., simply repeating an RF power measurement while the circuit topology and components are constant) can be very low, perhaps on the order of a hundredth of a dB; however, as explained above, there are systematic errors (typically Type B) that must be taken into consideration: for example the uncertainty of the waveguide coupling factor, impedance mismatches and other systematic biases. These types of errors cannot be reduced with repeated trials and averaging.

4.1 *An Engineering Calibration Uncertainty Estimate*

In this section the uncertainties of making waveguide power measurements are discussed and applied to the uncertainty budget for Eq. (3). Figure 8 shows a block diagram for a differential power measurement. In this setup (modeled after the ATE) a switch is used to select either the H or V waveguide for measurement. Shown also are circles that indicate some of the various uncertainties that affect power measurement. Table 1 gives a description of the uncertainties and typical values (2σ coverage, for high quality, well calibrated test equipment).

Assume that there are RF signals in the waveguides. To make a single power measurement (say from the H-waveguide), a waveguide coupler is used to extract power from the waveguide. The signal then passes through an attenuator, is converted to to a DC voltage which is then measured by the power meter. Each of the uncertainty factors along the electrical path, shown in Fig. **??** and numerically given in Table 1, are added in quadrature to ascertain the total uncertainty (quadrature is the square root of the sum of squares). When adding uncertainties in quadrature, the uncertainties are assumed independent. If it is suspected that the uncertainties are not independent and their relationship is unknown, then the uncertainties should be simply added which would yield a higher uncertainty than the quadrature addition (Taylor 1997). The estimated uncertainty of a single power measurement can be expressed

$$\begin{aligned} U_m^H &= f\big(U_c^H, U_{w,c}^H, U_{w,s}^H, U_s, U_{s,a}, U_a, \\ &\quad U_{a,p}, U_p, U_m\big). \end{aligned} \quad (4)$$

Using the values given in Table 1, the 2σ uncertainty is 0.195 dB.

For differential power measurements, some of the uncertainties will cancel, e.g., the uncertainties due to the attenuator, power sensor and power meter are common to both the H and V measurements and thus cancel in the ratio of H and V power measurement. The uncertainty of the differential waveguide power measurement can be expressed,

$$U_m^D = f\left(U_c^H, U_{w,c}^H, U_{w,s}^H, U_c^V, U_{w,c}^V, U_{w,s}^V\right) \quad (5)$$

where U_m^D is the differential power measurement uncertainty. Again, the uncertainties are assumed independent and are combined in quadrature to yield a total uncertainty of 0.183 dB.

This uncertainty can be regarded as an estimate of the uncertainty of the $\Delta(1,2)$ term in the EC calibration Eq. (3) where the transmit pulse power is measured at test plane 2 (the uncertainty of the power of the H and V transmit pulses is not included). If the same waveguide couplers are used to inject signals for the purpose of determining the $\Delta(2,4)$, more of these uncertainty terms in Eq. (5) will cancel when calculating the overall uncertainty of Eq. (3). Specifically, the uncertainty of the waveguide coupling factor, U_c, will cancel. However, additional uncertainty terms due to impedance mismatches are added.

- *An important observation is that the coupling factor for a waveguide coupler is bi-directional or reciprocal where as the associated impedance mismatch factors are not.*

Thus, if a signal is injected via the switch by a generator (gn) as shown in Fig. 8 for the purpose of measuring $\Delta(2,4)$, when calculating the uncertainty of Eq. (3), the waveguide coupler uncertainty factor will cancel; however, the uncertainties due to impedance mismatches will not cancel due to the non reciprocity of these factors. Thus, the direction of the RF signal is accounted for with the superscripts "inj" for inject a signal into the waveguide while "out" denotes that a signal is extracted from the waveguide. The total uncertainty of Eq. (3) can be expressed

$$\begin{aligned} U_m^T \quad = \quad & f\big(U_{w,c}^{H_{inj}}, U_{w,s}^{H_{inj}}, U_{w,c}^{V_{inj}}, U_{w,s}^{V_{inj}}, U_{w,c}^{H_{out}}, \\ & U_{w,s}^{H_{out}}, U_{w,c}^{V_{out}}, U_{w,s}^{Vout}, U_s, U_{gn}, \\ & U_{g,s}, U_{sun}, U_{tx}\big) \end{aligned} \quad (6)$$

where the "inj" is associated with the impedance mismatch at the waveguide coupler interfaces when signal is being injected into the waveguide, the "out" is associated with the impedance mismatch at the waveguide coupler interfaces when signal is being sampled from the waveguide. As can be seen from Eq. (6), the uncertainty of making a Z_{dr} bias estimate via Eq. (3) is due in large part to impedance mismatches. Other uncertainties are U_{gn} the signal generator, U_s switch jitter, U_{sun} sun variability and processing procedures (0.05 dB), and U_{tx} the power injection uncertainty for the measurement $\Delta(1,2)$ (0.05dB). The impedance mismatches are quite significant and the 2σ uncertainty estimate due to just just the 8 waveguide impedance mismatch terms is 0.186 dB (i.e., adding the 8 individual uncertainty estimates of 0.06 dB in quadrature). Adding the rest of the uncertainties yields $U_m^T = 0.192\,dB$. The uncertainties used are taken from Table 1 where we assume $U_{w,c}^{H_{inj}} = U_{w,c}^{H_{out}} = U_{w,c}^H$ and similarly for the other impedance mismatches.

a. *Impedance mismatch factors*

For each RF component interface a connection of some sort needs to be made and for each connection there will exist an impedance mismatch that will give rise to unknown reflected signal that will alter the power measurement causing measurement uncertainty. Each mismatch alteration is itself deterministic and may be corrected if the relevant scattering parameters of the junction are known, however this correction is complex.

In principle, it is possible via vector power measurements to determine the complex impedance seen at each junction and then use the measured complex impedances to correct power measurements. In practice this is not feasible especially for operational radars. Instead RF components are chosen to minimize such effects. For the uncertainty budgets presented here, we have estimated the the uncertainty due to impedance mismatch to be 0.06 dB. For more details on impedance mismatch see Dixon et al. (2007) and Kearn and Beatty (1967).

5. THE CROSSPOLAR POWER APPROACH

The CP method has been successfully applied to the CSU-CHILL radar data to calibrate Z_{dr} (Hubbert et al. 2003). The technique uses the property of radar reciprocity (Saxon 1955) which means that the off diagonal terms of the radar scattering matrix, S_{hv}, S_{vh}, are equal (Bringi and Chandrasekar 2001). Using this fact the Z_{dr} calibration equation can be derived:

$$Z_{dr}^{cal} = Z_{dr}^m S^2 \frac{\overline{P_{xv}}}{\overline{P_{xh}}} \quad (7)$$

where Z_{dr}^{cal} is calibrated Z_{dr}, Z_{dr}^m is measured Z_{dr}, S is the ratio of the V and H power from sun measurements, and $\overline{P_{xh}}$, $\overline{P_{xv}}$ are the average crosspolar powers for transmit H and transmit V polarization, respectively. The crosspolar powers may be averaged over a few rays or an entire volume of radar data. Both precipitation as well as ground clutter targets may be used. If precipitation targets are used, fast alternating H and V transmit polarizations must be used. The CP Z_{dr} calibration approach is like the VP technique in that neither require waveguide couplers, signal sources nor power meters and thus the associated uncertainty related to such RF measurements is eliminated.

S-Pol employs a copolar and crosspolar receiver design in contrast to H and V receivers. This is done to reduce the variance and drift of the Z_{dr} measurement but this also slightly changes the Z_{dr} calibration equation to:

$$Z_{dr}^{cal} = Z_{dr}^{m} S_1 S_2 \frac{\overline{P_{xv}}}{\overline{P_{xh}}} \tag{8}$$

where S_1 is the ratio of V-copolar to H-copolar sun radiation and S_2 is the ratio of V crosspolar to H crosspolar sun radiation (See Hubbert et al. 2003 for details).

6. EXPERIMENTAL RESULTS

In this section we present experimental results that are indicative of the uncertainty of the measurements that are required for the three Z_{dr} calibration techniques. Data come from both the RVP8 and VIRAQ processors. In the following analysis we assume that all systematic errors are negligible and thus we are estimating the uncertainty due to random errors. Any systematic error should be evident when the Z_{dr} biases calculated from the EC, CP and VP methods are compared.

6.1 *Sun Measurement Statistics*

Both the EC and CP calibration techniques require sun measurements. The sun radiation at S-Band is assumed unpolarized (Tapping 2001) and thus the H and V powers are equal. During high sun spot activity, there can be circularly polarized radiation also (Tapping 2001). However, circularly polarized radiation will also split equally into H and V polarized components.

By making passive sun measurement (i.e., the transmitter is turned off), the entire receive paths are calibrated. The sun power measurement are noisy and thus a sufficient number of samples need to be averaged in order to achieve a mean estimates that have low variance. A sufficient number of samples are gathered when scanning the sun slowly at about 1 deg. per second. Since the H and V antenna patterns are not matched exactly, it is important to average data over the a significant portion of the main beam rather than just using maximum values.

Typically the sun is scanned with one tenth degree elevation steps at about one degree per second rate. Obviously, the location of the one tenth of a degree separated elevation angle cuts through the sun will vary from one sun scan to another and this could affect the calculation of of the $S_1 S_2$ ratio needed for Z_{dr} calibration.

To reduce the sun integration errors, sun data points are first interpolated to a uniform rectangular $0.1^\circ \times 0.1^\circ$ grid. In order to determine the location of the sun center (considered the maximum power point), data along each of the vertical and horizontal grid lines are fitted to a Gaussian shaped curve and the location of the horizontal and vertical maximums of the Gaussian shaped curves are considered as the center of the sun. Note that the sun's center may not fall on on one of the grid points. The data is then integrated over different annuli corresponding to different solid angles. It has also been found that by using 3 consecutive sun scans to construct the grid of data, lower variances of $S_1 S_2$ is obtained. Before gridding the data, the sun's movement and elevation angle distortion must be accounted for.

On 21 June 2007, an entire day of sun box scans were made. The horizontal axis is labeled in "UNIX days". $S_1 S_2$ values are calculated by combining consecutive sets of 3 sun box scans. Fig. 9 shows the $S_1 S_2$ values for various integration annuli. For the annulus of 1.25 degrees, smallest variances are achieved this variance is about 0.01 dB over a short period of time (say about 0.5 hours) which give a 2σ uncertainty of about 0.02 dB. However, there is also a significant drift over the of nearly 0.1 dB. This indicates that the Z_{dr} bias should be monitored and corrected over a day's measurements. More about Z_{dr} bias correction is discussed later.

Such grided solar scan data can be used to construct pseudo antenna patterns. See Dixon et al. (2007) for more details.

6.3 *Vertical Pointing Measurements*

Vertical pointing measurements in rain have an intrinsic Z_{dr} of 0 dB when data is averaged over a 360° rotation of the radar dish (Bringi and Chandrasekar 2000). A measured non-zero value is considered the system Z_{dr} bias. To evaluate the uncertainty of the VP Z_{dr} bias estimate, 90 consecutive 360° vertical point scans were made in light rain on 23 May 2007 using RVP8. Each measurement results from integrating measured Z_{dr} over one 360° antenna revolution and using the following thresholds: range $>$ 2.7km, 30 dB$<$ SNR $<$60 dB, $\rho_{hv} > 0.95$ and $LDR > 20$ dB. Each 360° revolution takes about 1 minute. Fig. 10 shows the 90 Z_{dr} bias values in dB scale. The total extent of the vertical axis is 0.045 dB. There appears to be a mean increasing trend to the data set. If this trend is eliminated the the standard deviation of the de-trended data is about 0.01 dB which gives a 2σ uncertainty of of the Z_{dr} bias estimate of 0.02 dB. However, the trend in the data set again point to the necessity of monitoring the the Z_{dr} bias.

6.4 *Crosspolar Power Data*

In addition to the sun measurements, the CP technique for Z_{dr} calibration requires the measurement of the mean crosspolar power ratio, $\overline{P_{xv}}/\overline{P_{xh}}$. The CP technique takes advantage of the principle of radar reciprocity which dictates that the two crosspolar powers must be equal (there are materials that do not obey reciprocity such as ferrite but these types of materials are very rare radar targets). An interesting aspect of the principle of reciprocity is that is applies to the radar as a device; i.e., the entire radar antenna pattern is reciprocal so that the antenna sidelobes can not effect the measurement!

The NEXRAD dual polarization system will use simultaneous H and V transmission and reception and thus, near simultaneous samples of H and V crosspolar returns will not be available. However, if two slow waveguide switches are used then the NEXRADs will be able to measure both crosspolar powers. One technique for the evaluation of $\overline{P_{xv}}/\overline{P_{xh}}$ is to alternate between only H and only V transmission on a PPI to PPI basis. If the beams are indexed, crosspolar powers from the same resolution volumes (but from different PPI scans) can be paired and used for the CP calibration. Another viable technique is to simply point the radar along a radial where there are good clutter targets. The slow wave guide switch can alternated H and V transmit polarization that illuminate the same clutter targets.

On 18 October 2006 the PPI measurement technique was tested using RVP8 data. PPI scan data were collected in fast alternating transmit H and V mode, followed shortly by H-only transmit, and then V-only transmit modes. The crosspolar power ratios were calculated from both sets of data. For 22 H and V PPI pairs, the mean crosspolar power ratio is $\overline{P_{xv}}/\overline{P_{xh}} = 0.373\,\mathrm{dB}$ with a 2σ uncertainty of 0.032 dB. Similarly, for the fast alternating mode, the mean $\overline{P_{xv}}/\overline{P_{xh}} = 0.404\,\mathrm{dB}$ and the 2σ uncertainty is 0.002 dB. The uncertainty of $\overline{P_{xv}}/\overline{P_{xh}}$ for the fast alternating method is much lower than that for the alternate H and V PPI method; however, these results show that the cross polarization approach is amenable to NEXRAD.

6.5 *Comparison of Calibration Techniques*

The Z_{dr} calibration factor or bias of the S-Pol system should be the same whether using the VP, the CP or EC techniques. The following data were gathered on 31 August 31 2006 but are representative, in general, of our calibration measurements. The Z_{dr} bias calculated from VP data is $0.712\,\mathrm{dB}\pm0.019\,\mathrm{dB}$. The Z_{dr} bias is calculated via the CP technique using Eq.(8) from sun measurements and crosspolar power measurements, also gathered on 31 August 2006. S_1S_2 is -1.051 $\mathrm{dB}\pm0.013\,\mathrm{dB}$ while the crosspolar power ratio was -0.323 $\mathrm{dB}\pm0.014\,\mathrm{dB}$. This yields a Z_{dr} bias of $(-0.323) - (-1.051) = 0.728\,\mathrm{dB}\pm0.027\,\mathrm{dB}$ which is in excellent agreement with the VP bias estimate $0.712\,\mathrm{dB}\pm0.019\,\mathrm{dB}$. Both of these uncertainties are derived from Type A evaluations. There are likely other systematic errors that we have neglected for both techniques. For the VP we estimate these neglected errors to contribute an uncertainty of 0.05 dB. For the CP technique, we estimate an uncertainty of 0.05 dB for both the crosspolar power ratio $\overline{P_{xv}}/\overline{P_{xh}}$ and the sun ratio measurement S_1S_2. These neglected Type B errors could arise from the data processing techniques, sun scan anomalies or other unidentified influence factors. An example of such anomalies is given in the next section. This then changes the VP bias estimate to $0.712\,\mathrm{dB}\pm0.053\,\mathrm{dB}$ and the the CP estimate to $0.728\,\mathrm{dB}\pm0.075\,\mathrm{dB}$. Both 2σ uncertainties are still under the 0.1 dB requirement. The results from the EC approach indicate Z_{dr} measurement bias is 0.80 dB with a total uncertainty of about 0.25 dB (other uncertainties are are included in this estimate that were not included in Section 4.1 above). The EC bias number of 0.80 dB was estimated from data taken over several days so that a direct comparison of the EC bias to the CP and VP biases is not warranted. The uncertainty estimate of the EC bias, 0.25 dB, however, more importantly indicates that the EC Z_{dr} bias may not be estimated to within the 0.1 dB requirement.

7. $\mathbf{Z_{dr}}$ MONITORING

As indicated by the above data, the Z_{dr} bias is very likely to drift significantly during the course of a day. These drifts, though small, are on the order of a tenth of a dB, for the S-Pol system, and thus the Z_{dr} bias needs to be monitored and the Z_{dr} bias adjusted. The components most prone to gain drift are the active components, i.e., the LNAs and the receiver. This active portion of the receiver path can be monitored for gain drifts by 1) injecting test pulses at test plane 3 (see Fig. 7) and measuring the resulting differential power at the I&Q samples and 2) scanning the sun. Obviously the sun is not always available to be scanned so that test pulse injection is preferable. However, the sun should be scanned as as often as practical for a redundancy check. In the following two data sets, the sun scan data are compared to test pulse injection data.

Fig. 11 shows S_1S_2 sun scan numbers (in purple) versus time in Unix days for 17 July 2007. The horizontal axis extent is 14.4 hours and the vertical axis is in dB.

The sun scan numbers are calculated from a single sun box scan. The blue markers show the drift in S_1S_2 as measured via test pulse injected at measurement plane 2. Both data sets show the same trends with the test pulse measurements showing less variance. The sun scan measurement variance could be reduced if 3 box scans were used to calculate S_1S_2. At the beginning of the plot, the average difference between the two data sets is about 0.03 dB where as the average difference grows to about 0.08 dB at Unix time 37818.75. This discrepancy could be due to 1) the processing algorithm of the sun data, 2) unaccounted variations in the sun as an unpolarized source 3) other unaccounted variances in the electrical path. Consider the third alternative. The test pulses only monitor the gain drifts from measurement plane 3 to the I&Q samples. The sun measurement plane take into account the entire receive path from outside the antenna to the I&Q samples. Thus, there could be gain fluctuations cause by the electrical path from the antenna to measurement plane 3 that could account for the differences seen in Fig. 11. Such discrepancy illustrate the difficulty in making RF power measurements accurate to sub tenth of a dB levels and to the realistic evaluation of RF power measurement uncertainty at these levels.

Fig. 12 shows similar S_1S_2 data as shown in Fig. 11 for 21 June 2007. Again there is a differential discrepancy of about 0.08 dB between the curves from the beginning of the data set to Unix time 37792.7. This is of the same magnitude and direction as seen in Fig. 11. Thus it is unlikely that the sun processing algorithm is responsible for the observed discrepancy. One explanation is that via heating by the sun, the electrical path from the antenna to measurement plane 3 is altered via expansion. This then appears to point to another RF power measurement uncertainty source. Further measurements and investigation are needed.

8. CONCLUSIONS

NCAR conducted an experiment for OS&T of NOAA/NWS to evaluate Z_{dr} calibration techniques for the WSR-88Ds using S-Pol, NCAR's S-band polarimetric radar. Three techniques for Z_{dr} calibration were investigated: 1) vertical pointing (VP) data in light rain, 2) engineering calibration technique (EC) and 3) the crosspolar power technique (CP). Measurement and analyses were performed in order to quantify the uncertainty of the estimated calibration numbers and the measurement procedures that yield such uncertainty. The uncertainty of measurements can be separated into two categories: 1) systematic and 2) random. VP measurements in light rain are widely regarded as the most accepted way to calibrate Z_{dr} and such measurements were used to truth other Z_{dr} calibration measurements. Several sets of VP data were gathered over the the summer of 2006 and 2007 and analysis showed that the Type A uncertainty of the VP Z_{dr} calibration was on the order of 0.02 dB. Again, this is an evaluation of the *random measurement errors* and possible systematic biases may be present, e.g. due to data processing. A main objective of this Z_{dr} calibration experiment is to determine the uncertainty associated with the EC Z_{dr} calibration technique. The uncertainty of the EC technique was established via both Type A and Type B uncertainty evaluations. The S-Pol Z_{dr} bias calculated for the EC technique was measured to be about 0.80 dB with an uncertainty estimated to be about 0.25 dB (2 σ coverage). The 0.25 dB uncertainty number is dominated by impedance mismatches. In general, the EC technique yielded Z_{dr} biases about a tenth of a dB higher that the VP and CP techniques.

Evaluation of sun measurements impacts both the EC technique as well as the CP technique. The sun's radiation (at S-band) can be considered unpolarized and thus the power of the sun is equally divided between horizontal (H) and vertical (V) polarizations. Solar flares can create polarized radiation but is typically circular polarization which also provides equal powers between the H and V channels. Thus, the sun's radiation is an good RF source for the evaluation of the differential gain of a radar's H and V receive channels. However, great care must be taken in the processing of such sun scan data sets. The sun data should be interpolated to a grid with the sun movement and elevation angle angle distortion accounted for. Accurate noise correction needs to be made and sufficient sun data must be averaged to to reduce measurement random error. Day long measurements of sun show that the Type A uncertainty of S_1S_2 measurements is on the order of 0.02 dB for sufficient averaging.

Measurements with S-Pol thus far have shown excellent agreement between the Z_{dr} bias found via VP measurements and the CP techniques (e.g., biases are typically are within 0.03 dB of each other). Both techniques yielded Z_{dr} bias uncertainties within the desired uncertainty limit of 0.1 dB. Additionally, it was shown that the CP technique can successfully be employed on radar systems that achieve dual polarization measurement via simultaneous transmission of H and V polarizations as NEXRAD will do (i.e., such radars typically do not have a fast polarization switch). For this transmitter topology, slow waveguide switches can be used to gather alternate PPIs of transmit only H and transmit only V data. Using indexed beams, the transmit H and transmit V crosspolar powers from the alternate PPIs were equated. This can done with many ground clutter targets since the backscatter cross sections of stationary ground clutter targets is invariant. These results indicated that the crosspolar technique could be used with NEXRAD type radars.

In order to assure Z_{dr} measurement accuracy to better than a tenth of a dB uncertainty, the active portion of the receiver chain needs to be monitored. Two differential gain monitoring techniques were examine: 1) test pulse injection and 2) sun scan measurements. They tracked each other fairly well but differential gain drift between the two measurements varied as much as 0.08 dB during day long measurement periods. This may indicate another systematic error source that needs to accounted for.

A main conclusion of this study is that the 2 σ uncertainty of the EC Z_{dr} bias measurement is approximately 0.25 dB which exceeds the 0.1 dB specification requirement. The uncertainty is dominated by impedance mismatches. Reduced uncertainty could be achieved if meticulous vector power measurements were made that could quantify the inevitable impedance mismatches that occur but this is deemed to be impractical for operational radars. To estimate Z_{dr} bias to within 0.1 dB uncertainty, some sort of "end-to-end" measurement technique is needed such as vertical pointing data in light rain or the crosspolar power technique which uses sun measurement in conjunction with crosspolar power measurements. No power meters or other RF sources are required which give rise to unacceptable uncertainty levels.

Acknowledgment
This work was supported by the Office of Science and Technology of the National Weather service. The authors would like to acknowledge the EOL/RSF technical staff for their time, effort and interest in the collection of the experimental data used in this paper. The National Center for Atmospheric Research is sponsored by the National Science Foundation. Any opinions, findings and conclusions or recommendations expressed in this publication are those of the author(s) and do not necessarily reflect the views of the National Science Foundation.

References

Bringi, V. and V. Chandrasekar, 2001: *Polarimetric Doppler Weather Radar*. Cambridge Univ. Press, Cambridge, UK.

Dixon, M., J. C. Hubbert, S. Ellis, C. Kessinger, and G. Meymaris: 2007, Intelligent mitigation of normal propagation and anamolous propagation clutter. *Preprints of 33rd AMS Conf. on Radar Meteorology*, Cairns, Australia.

Doviak, R., V. Bringi, A. Ryzhkov, A. Zahrai, and D. Zrnić, 2000: Polarimetric upgrades to operational WSR-88D radars. *J. Atmos. Oceanic Technol.*, **17**, 257–278.

Hubbert, J.C., V.N. Bringi and D. Brunkow, 2003: Studies of the polarimetric covariance matrix: Part I: Calibration methodology. *J. Atmos. and Oceanic Technol.*, **20**, 696–706.

Jursa, A.S. (Editor) , 1985: *Handbook of Geophysics and the Space Environment*. National Technical Information Service, iSpringfield , VA, 4 edition.

Kearn, D. and R. Beatty, 1967: *Basic Theory of Waveguide Junctions and Introductory Microwave Analysis*. Pergamom Press.

Kraus, J.D. , 1986: *Radio Astronomy,*. Cygnus-Quasar Books, 2^{nd} edition.

Saxon, D.S., 1955: Tensor scattering matrix for the electromagnetic field. *Phys. Rev.*, **100**, 1771–1775.

Tapping, K.: 2001, Antenna calibration using the 10.7 cm solar flux. *Radar Polarimetry for geoscience applications*, P. Smith, ed., American Meteorological Society, http://cdserver.ametsoc.org/cd/010430_1/RADCAL_Links_2_Presentatio

Taylor, J., 1997: *An Introduction to Error Analysis*. University Science Books, Sausalito, CA.

Taylor, B.N., and C.E. Kuyatt, 1994: Guidelines for evaluating and expressing the uncertainty of NIST measurements results. Technical report, US Dept. of Comm. National Institute of Standards and Tech., note 1297.

Technologies, A., 2001: Fundamentals of rf and microwave power measurements. Technical report, Agilent Technologies, application Note 64-1C.

Zrnić, D.S., V.M. Melnikov, and J.K. Carter, 2006: Calibrating differential reflectivity on the WSR-88D. *J. Atmos. and Ocean. Tech.*, **23**, 944–951.

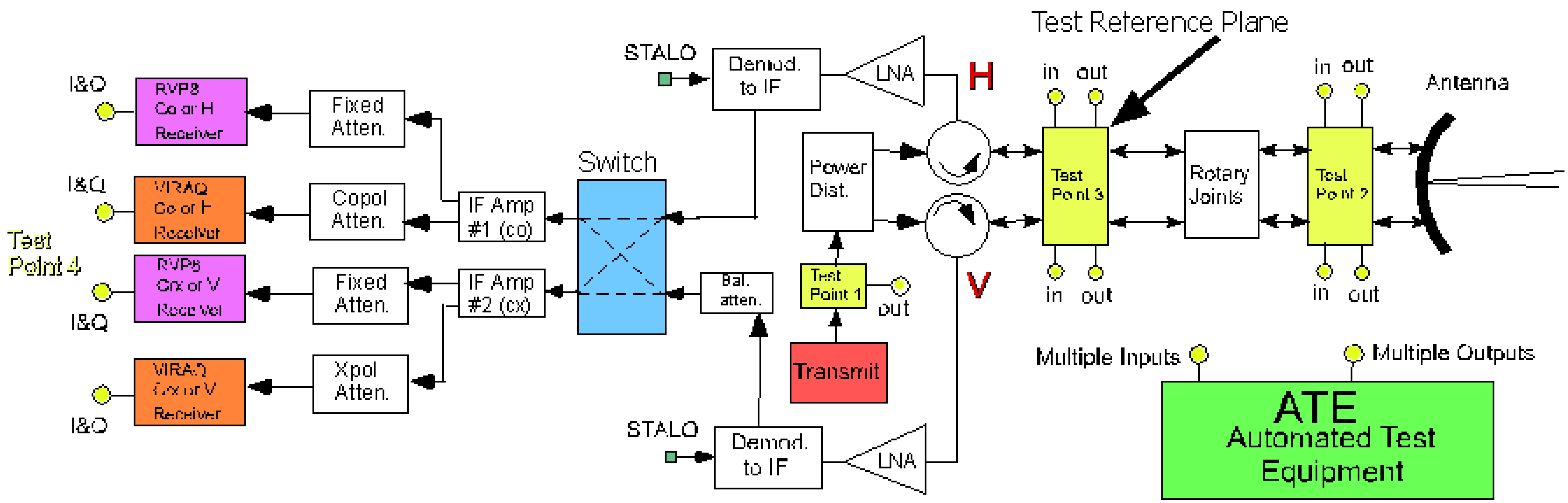

Figure 1: *A block diagram of S-Pol showing the Automated Test Equipment.*

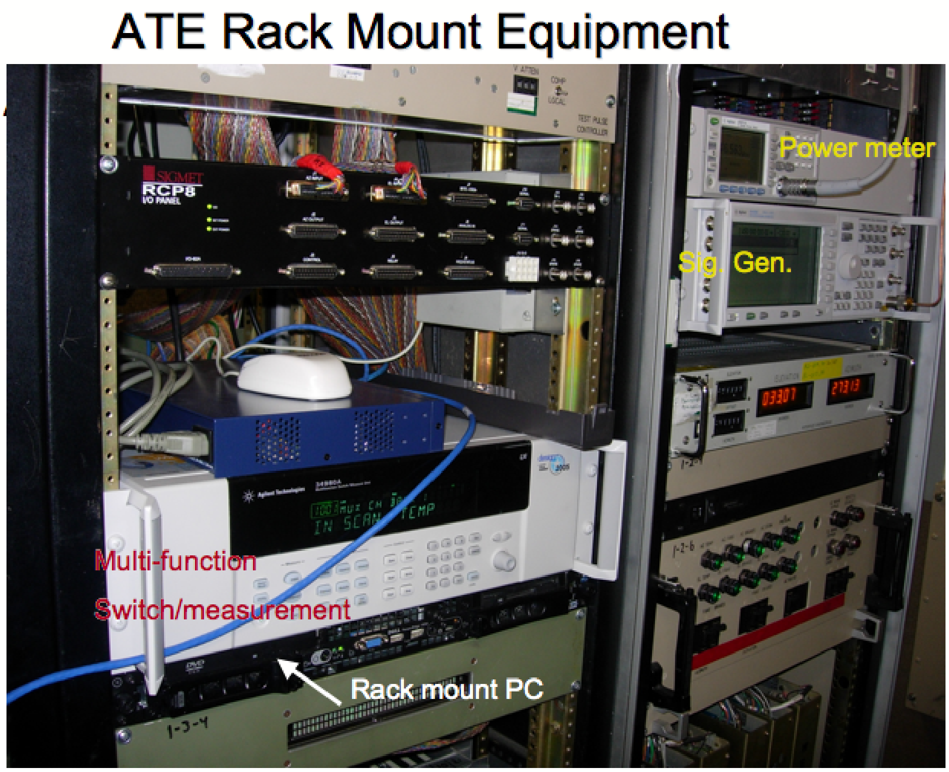

Figure 2: *Part of the ATE test equipment mounted inside the S-Pol transmitter trailer.*

Uncertainty	**Description**	**value (dB)**
U_s	Waveguide coupling factor	0.1
U_s	Switch	0.01
U_a	Attenuator	0.08
U_p	Power sensor (RF to DC)	0.09
U_m	Power meter	0.05
$U_{w,c}$	Impedance mismatch between waveguide coupler and waveguide	0.06
$U_{c,s}$	Impedance mismatch between waveguide coupler and switch	0.06
$U_{s,a}$	Impedance mismatch between switch and attenuator	0.06
$U_{g,s}$	Impedance mismatch between generator and switch	0.06
U_{gn}	generator noise	0.02
U_{gn}	Sun source & processing	0.05

Table 1: *A list of 2σuncertainties for the differential power measurement shown in Fig. 8 .*

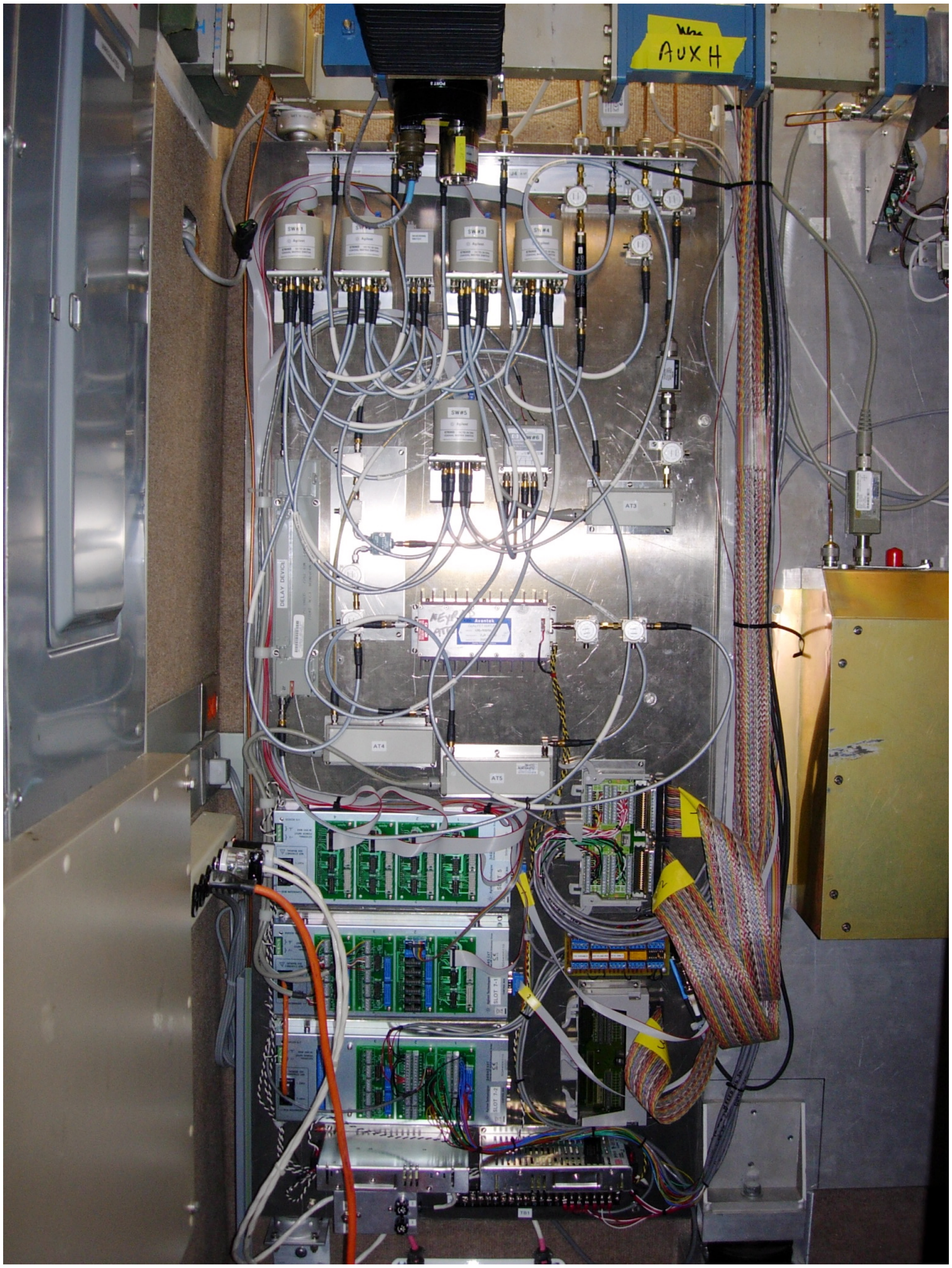

Figure 3: *Part of the ATE test equipment mounted inside the S-Pol transmitter trailer .*

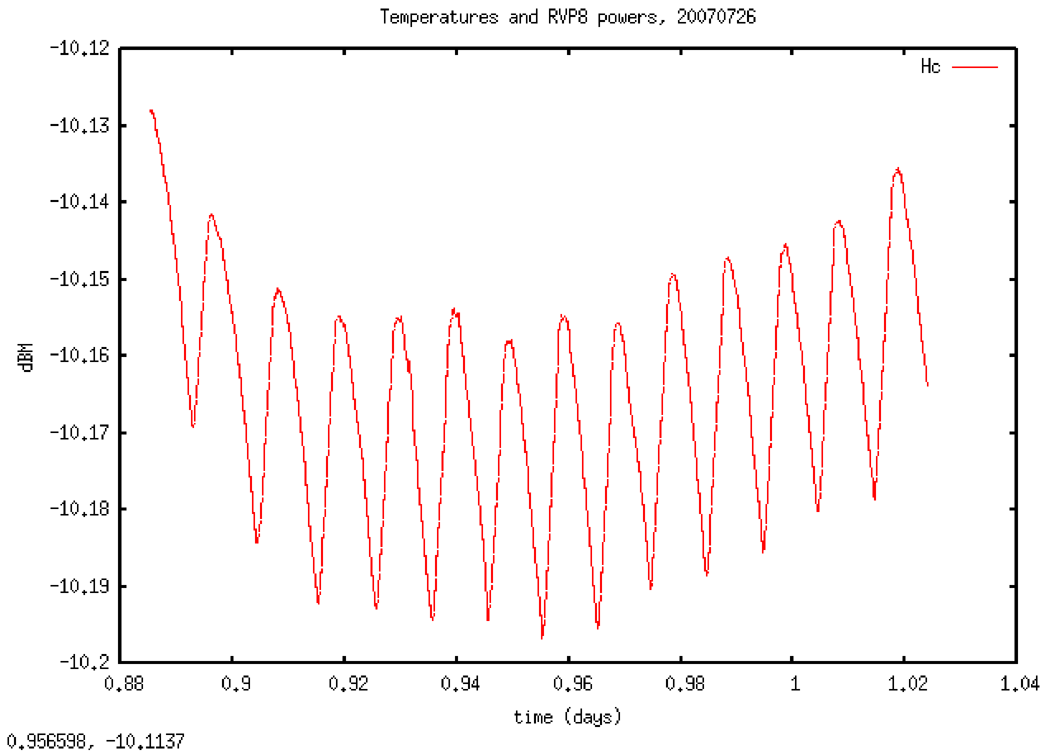

Figure 4: *The H channel power as a function of time as measured by the ATE for a constant CW input.*

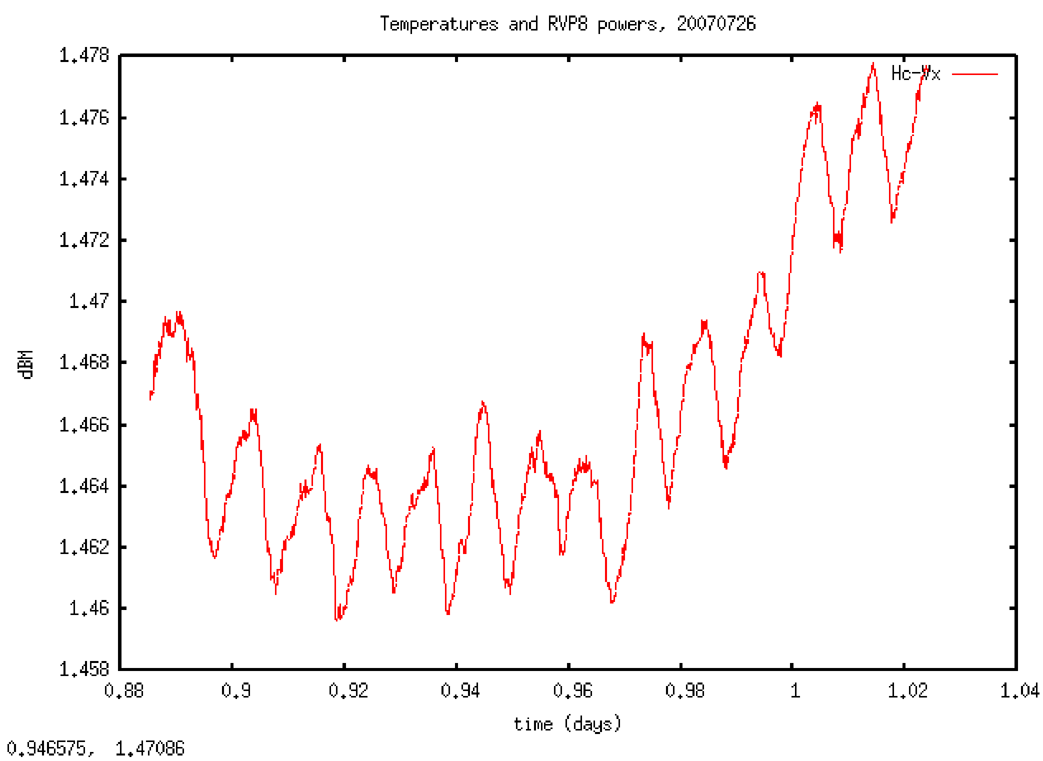

Figure 5: *The H copolar power minus the V crosspolar power in dB as a function of time in fractional days.*

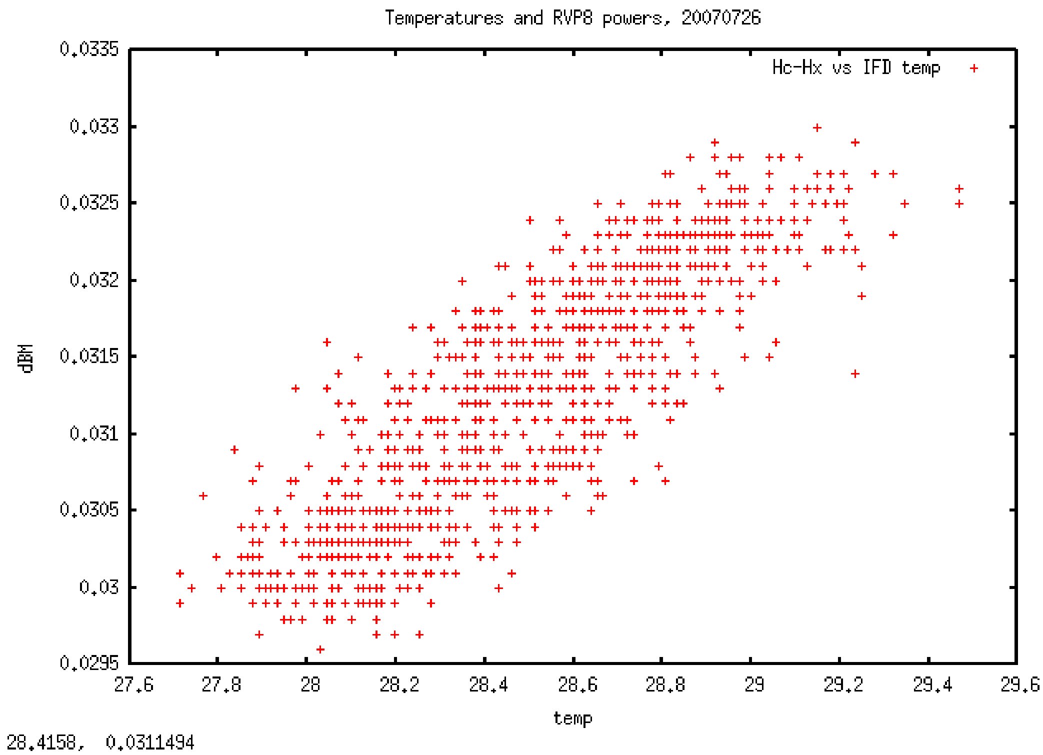

Figure 6: *H copolar power minus H crosspolar power in dB versus IFD temperature in Celsius.*

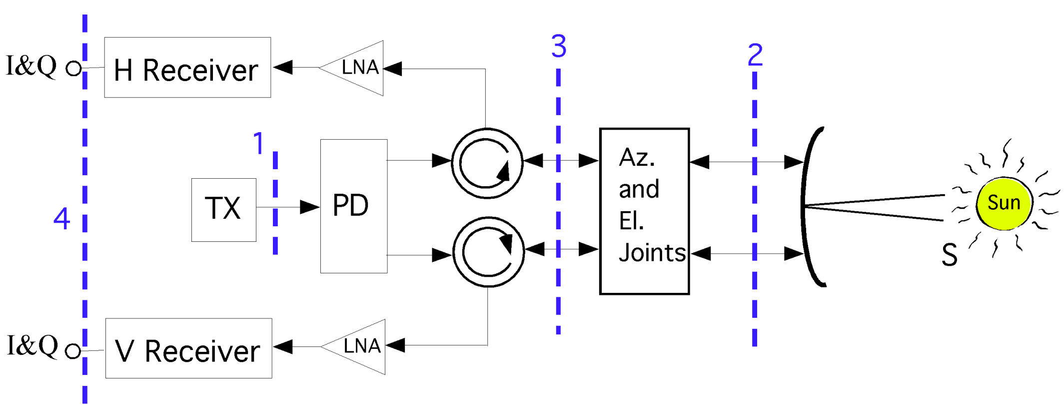

Figure 7: *A block diagram of a radar system for the EC method.*

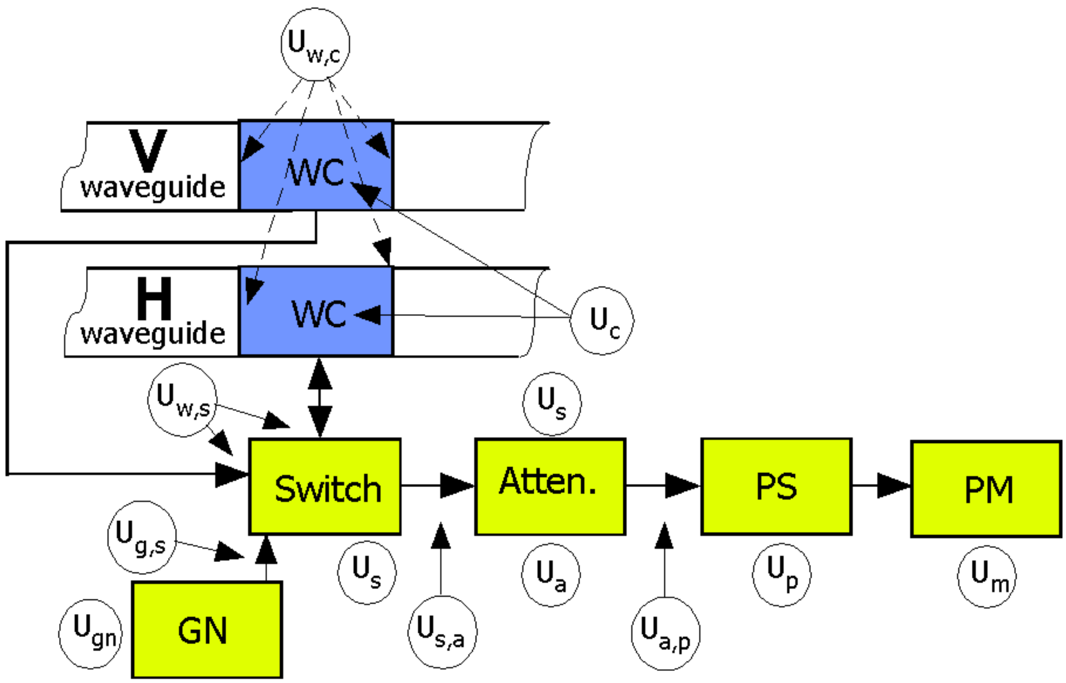

Figure 8: *A block diagram of a differential waveguide power measurement. "WC" is waveguide coupler, "Atten." is an attenuator, "PS" is a power sensor, "PM" is a power meter and "GN" is a generator. The circles represent the various uncertainties. The double subscripted uncertainties are various impedance mismatches between the devices. A list of the uncertainties with definitions is given in Table 1*

Figure 9: S_1S2 *sun scan measurements over an entire day for various solid angles of integration.*

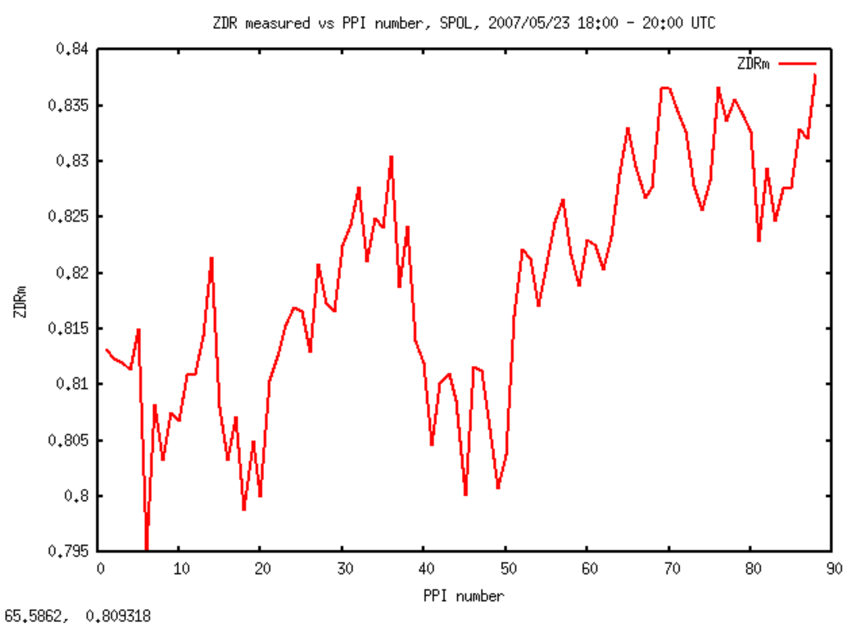

Figure 10: Z_{dr} *biases calculated from 90 consecutive 360° vertical pointing scans. There is one estimated bias per 360° scan.*

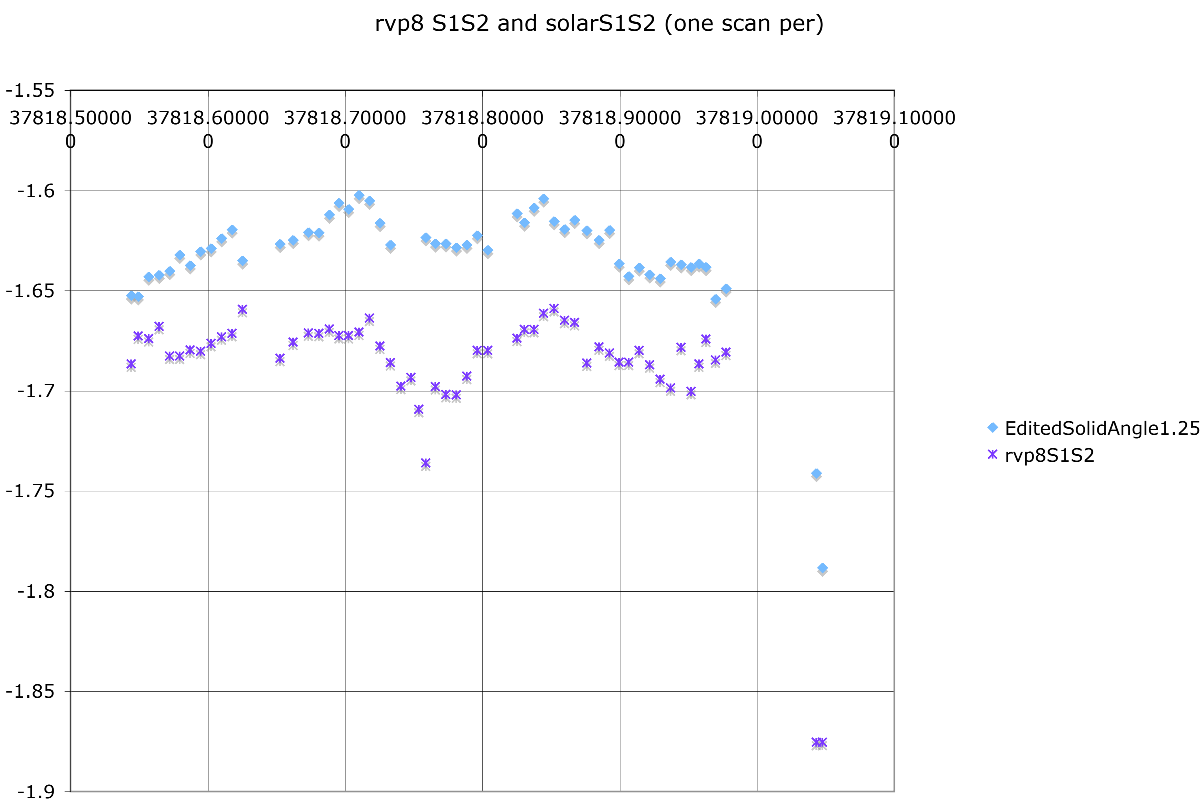

Figure 11: *A comparison of Z_{dr} bias monitoring via test pulse injection (purple markers) and sun scans (blue markers). The horizontal axis is in Unix days and the vertical axis is in dB. Data was gathered on 17 July 2007.*

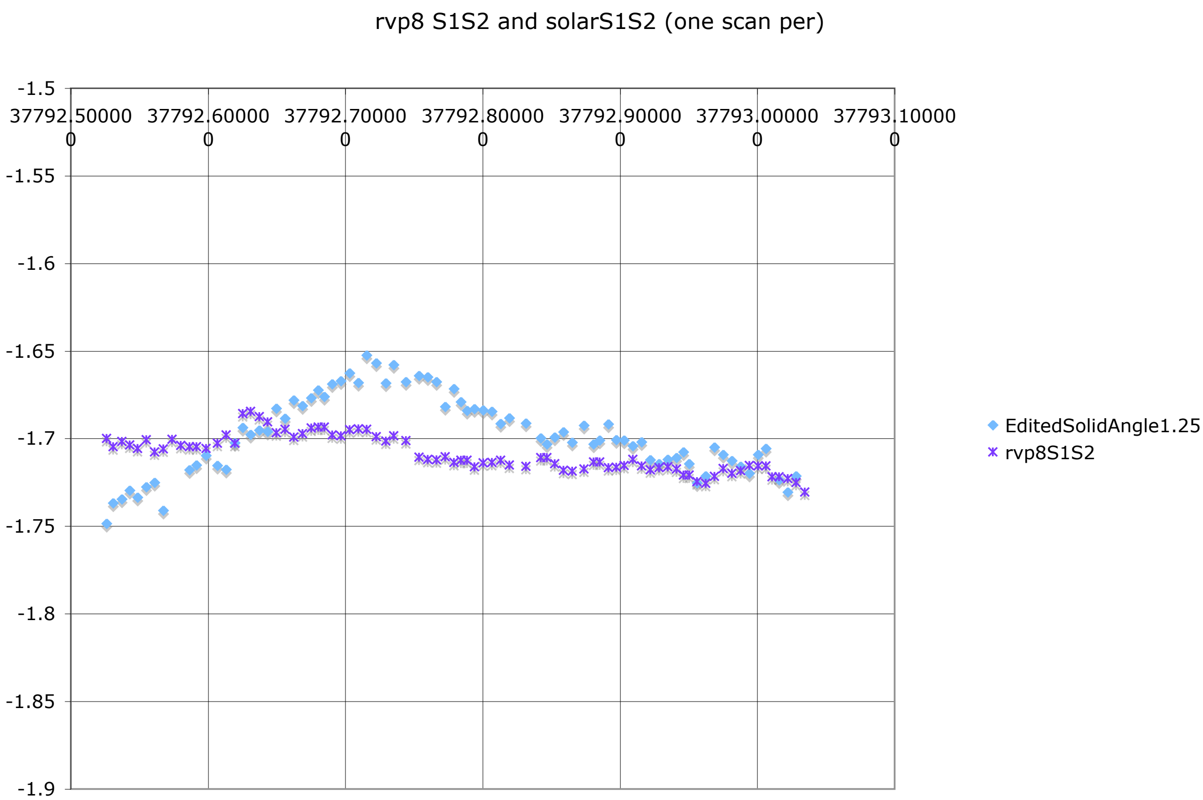

Figure 12: *A comparison of Z_{dr} bias monitoring via test pulse injection (purple markers) and sun scans (blue markers). The horizontal axis is in Unix days and the vertical axis is in dB. Data was gathered on 21 June 2007*